High Energy Probes

A. Bonasera, R. Coniglione and P. Sapienza

INFN - Laboratori Nazionali del Sud, Via S. Sofia 62, 95123 Catania (Italy)

Abstract. We review some results on energetic particles production in heavy ion collisions below roughly 100 MeV/A both theoretically and experimentally. We discuss the possibility to gather information about the nuclear Equation Of State (EOS) and viscosity from data. Results on subthreshold pion, energetic photons and nucleons are discussed and contrasted to microscopic models. Important information about the first stages of the reaction are obtained by such probes. At present, we can conclude that we have at least a qualitative understanding of the processes involved when such particles are produced. However, a quantitative understanding of the data and the possibility of understanding deeply the formation mechanism, i.e. incoherent, cooperative or statistical, plus the derivation of important properties of the nuclear EOS are still missing. This calls for new data using more modern detector systems and comparison to more refined microscopic models.

Keywords: Enter Keywords here.
PACS: Replace this text with PACS numbers; choose from this list: **http://www.aip.org/pacs/index.html**

INTRODUCTION

One among the many purposes to collide heavy ions at beam energies below 100 A·MeV is the study of the nuclear matter equation of state (EOS) at finite densities and temperatures. In fact, in such conditions the two nuclei, initially in their ground state, are compressed and heated up. After tens of fm/c, the maximum compression is reached and a compound is formed which then expands and depending on the excitation energy reached might even break into many pieces (multi fragmentation). In such a scenario there are many factors at play. In the compression stage it is very important the EOS of the system and the viscosity. Thus data sensitive to the early stages such as energetic protons, neutrons and more complex fragments, as well as photons and pions, will give valuable information and put constraints on the EOS.

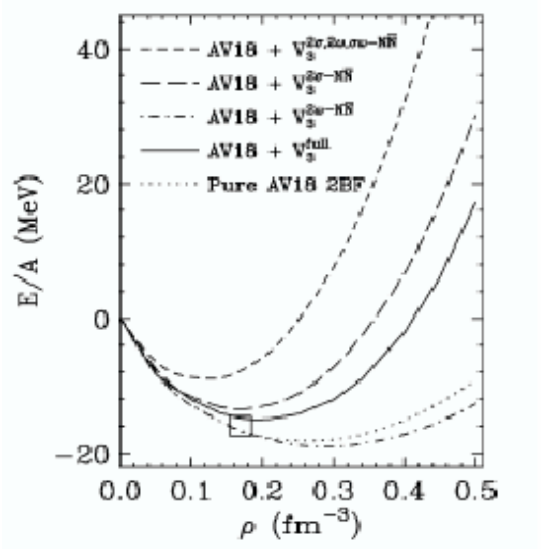

Fig.1 - BHF calculations of the nuclear matter EOS including three body forces. Binding energy per nucleon is reported as a function of density [**8**Lomb02].

In the intermediate energy regime, the powerful detection systems available (MEDEA [**1**Migneco92], INDRA [**2**Pouthas95], NIMROD [**3**Wada04], CHIMERA [**4**Pagano01], TAPS [**5**Martinez97]), MINIBALL [**6**Desouza90], MULTICS [**7**Iori93] (see chapter "Detection") allow to study with great accuracy energetic and subthreshold particles emission. The comparison of the particle emission characteristics (the dependence of the multiplicity on the impact parameter, the excitation energy removed, the angular distributions, the slope of energy spectra ….) with the prediction of transport models can put constraints on

the knowledge of the basic properties of hadronic matter as the in medium Nucleon-Nucleon cross section, nuclear matter compressibility, mean field properties, the relevance of two body versus three body forces etc…). It has been shown, for example, that the interplay between two and three body forces is very subtle and it turns out that to fit the ground state properties of nuclear matter in non relativistic microscopic calculations, it is necessary to introduce a three body force [**8**Lomb02]. This is demonstrated in Fig.1 for microscopic Bruckner Hartree Fock (BHF) calculations [**8**Lomb02] where the binding energy per nucleon is reported as a function of the density of nuclear matter at finite temperature. In the figure, the calculations with only two body forces are given by the dotted line. The two body force is parameterized to fit the nucleon-nucleon data. We clearly see that the approach does not work, in fact it gives a ground state density of about 0.3 fm^{-3} and a binding energy of about -20 MeV, while the experimental data is 0.15 fm^{-3} and –16 MeV respectively (square symbol in Fig.1). In order to improve the agreement to data, a genuine three body force was included in the calculations. The contribution from different channels are displayed in the figure and the final result is given by the full line. The effect is indeed dramatic. The ground state density is shifted to 0.19 fm^{-3} and the binding energy to the experimental value. The three body force is obtained through a fit to the binding energies of light nuclei, t and ^{3}He essentially [**9**Kievski04] but the one reported in Fig.1 is obtained by the meson-exchange model of Fujita-Miazawa [**8**Lombardo02]. In the nuclear matter calculations there are no adjusted free parameters. The fact that the calculations are not yet perfect implies that something is still missing. Some light on this problem could be given by experimental data on nucleon production in heavy ion collisions. We will show below that such data does not support the need for a strong three body force.

The equation of state discussed so far is at zero temperature. A complete knowledge of the EOS requires, however, information at finite temperatures. Microscopic calculations performed at finite temperatures show, as expected, that the EOS of nuclear matter looks like a Van Der Waals (VDW) EOS. In fact the nucleon-nucleon force has an attractive tail and a repulsive hard core such as many classical systems. At variance with classical systems the ground state is not a solid but a particular Fermi liquid. However, other properties such as liquid to gas phase transition at finite temperatures and small densities, are of the VDW type [**10**Bonasera00]. An important feature that makes nuclei different from classical system is the strong momentum dependence of the mean field. Microscopic BHF calculations gives strong indications on how the momentum dependence force should look like in nuclei and nuclear matter. Typical results of non relativistic BHF calculations are given in Fig.2 where the potential for protons are reported as a function of the nucleon momentum transfer for two different NM densities [**8**Lombardo02]. Also in this case the difference between 2 and 3 body forces is large especially near the Fermi momentum region at higher densities. Notice the difference between two and three-body forces at the two different densities. These features might be revealed through a careful analysis near the Fermi energy for the first case while at higher incident energies in the second one.

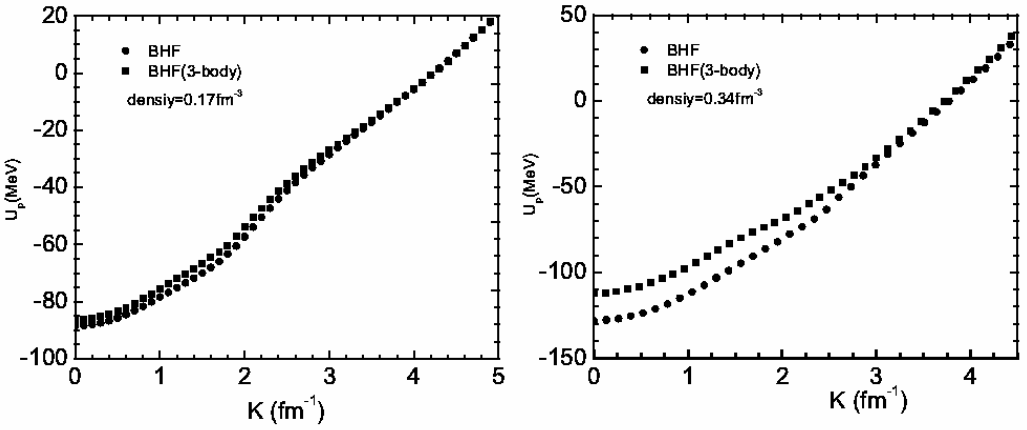

Fig.2 – BHF calculations. The proton potentials are reported as a function of the proton momenta at two different NM densities

In order to study the momentum dependence of the nuclear mean field we could resort again to heavy ion collisions. We have already many findings coming from electron scatterings [**11**povh]. However, in those experiments the mean field can be only tested at ground state densities and approximately zero temperature, which is relevant for the results of Fig. 2 left panel. At variance, in a heavy ion collision, depending on the beam energy, both density and temperature can be changed and undergoing to an initial non equilibrium stage. The duration of such a

stage, and the same possibility of reaching equilibrium depends on the properties of the mean field and on incoherent nucleon-nucleon collisions or even on higher order correlations. As we have outlined above the relevance of nucleon-nucleon collisions can be seen in proton experiments [**12**Coniglione00, **13**Sapienza01]. The momentum dependent force and the compressibility of EOS could be inferred, or at least strong constraints could be put to them, from subthreshold production of pions, gammas and energetic particle emission. This is a reason why we will restrict our work at energies below roughly 100 A·MeV, where non nucleonic degrees of freedom (such as delta excitation) are not so relevant yet. This energy region, we believe, carries important information on the EOS near the ground state density and moderate temperature. In Fig. 3 the maximum and average densities estimated by VUU calculations for central collisions as a function of the incident energies are reported for the $^{40}Ca + ^{40}Ca$ reaction [**14**cass90]. The comprehension of nuclear matter properties at moderate densities are crucial if we want to understand the EOS even at higher densities and temperatures where other degrees of freedom become relevant. We expect that other authors will discuss in detail experimental results and models at higher energies (GSI regime, see chapter "Systematics on Stopping and Flows"). In particular, in our contribution, we will not discuss the kaon and η production because they have been mainly studied at energies much higher than 100 A·MeV.

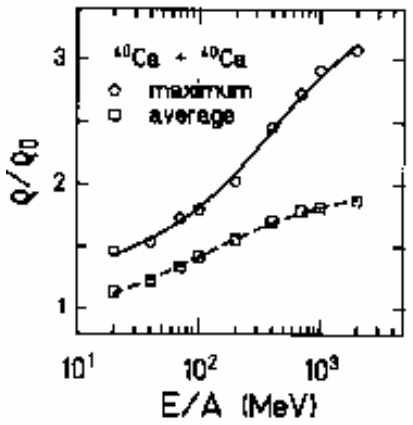

Fig. – 3 –Maximum and average densities as a function of the bombarding energy per nucleon as estimated by VUU calculations for central $^{40}Ca + ^{40}Ca$ reaction [14Cassing90].

The understanding of the EOS in the region of our interest has to go step by step with the elaboration of microscopic models. While some features of the EOS can be obtained directly from the data, a more qualitative understanding of nuclear properties must be obtained from a detailed comparison among models and data. For instance, we expect that energetic photon and pion production must be very sensitive to the momentum dependent part of the mean field. In fact, assuming incoherent nucleon-nucleon collisions, the final momenta of the colliding nucleons after producing a pion or a photon are decreased. This results in a strong (repulsive) mean field which acts against the production of the new particle essentially because of Pauli blocking, i.e. the colliding nucleons must provide energy to produce the new particle and to surmount the repulsive field. Thus their final momenta are reduced and they must not be Pauli blocked, otherwise the collision is not allowed. Unfortunately, we have not been able to find in the literature microscopic calculations of subthreshold particles production with momentum dependent forces in our region of interest. Many calculations exist for nucleons or more complex particles spectra and as a general feature a reduction of incoherent nucleon-nucleon collisions has been found with momentum dependent forces. Comparison of yields and slopes of energy spectra of energetic protons with predictions of transport models that include a local and a momentum dependent potential have been published and will be discussed later on in this chapter. If one extends this result to subthreshold particle production a difference of the calculated yield, compared to the results for momentum independent forces, is expected. This aspect should be carefully (re)analyzed also for π and hard photon production.

Most of the microscopic calculations, Boltzmann or molecular dynamics type [**15**Bonasera94, **16**Bertsch88, **14**Cassing90, **17**Aichelin91] have essentially two ingredients. One is the mean field which is parametrized to fit some general results such as electron scattering data, ground state properties of nuclei etc.. The other feature is a collision term which is composed of a probability inferred from NN data and a Pauli blocking which forbids that particles undergoing an elastic or inelastic scattering end up in a occupied state. These two ingredients of the models are usually uncoupled while it is clear that they should come from the same microscopic interaction. Few attempts exist to date to calculate these ingredients microscopically from the same interaction and to implement them in a transport code (see chapter on Modelization of EOS). The phenomenological approach underlined above is often used and one tries to put constraints from a comparison to data. The problem is that most often data is sensitive to both ingredients and it is not easy to disentangle them. However, a systematic comparison of the models to the data should put some constraints on the mean field and the collision term which are included in the calculations. This could be obtained if all the 'hidden' ingredients entering the models are under control, in fact, particles production is sensitive not only to the ingredients discussed above but also to the way the nucleus is prepared. To be more precise:

- In transport approaches one represents nucleons via test particles which could be one (molecular dynamics) (QMD,FMD,AMD,CoMD) or N_{tp} per particle (one body models, BUU, VUU, LV, BNV) and could have

particular representations, i.e. gaussian, delta functions, etc. The properties of the ground state of the nuclei depends on the choice one makes and the EOS could also be different even though one starts nominally from the same Skyrme type mean field.

- In the models different ways to define the ground state are used. In pioneering approaches a Fermi gas model was used, i.e. depending on (local) density a corresponding Fermi momentum is given to the test particles. This is not self consistent and more recent approaches (FMD,AMD, CoMD, BNV with constraint) implement some minimization procedure for the ground state of nuclei.
- Depending on the form used to represent the test particles one ambiguity results on calculating the Fermi energy. For delta function test particles the Fermi motion is given by the kinetic energy of the test particles. If one uses gaussian representation, then part of the Fermi motion could be given by the width of the gaussian. A consequence could be that if the width in momentum space of the gaussian is of the order of the Fermi momentum (as it is in many approaches) then the centroids of the Gaussians are essentially at rest which could imply that the system is a 'solid' in the ground state, i.e. if one plots just the positions of the gaussians versus time they remain at rest at all times. A careful analysis for example through the determination of the Lyapunov exponents might reveal a transition from 'solid' to 'liquid'. Even though this unwished feature could be avoided by dividing the Fermi motion between the width of the gaussian in momentum space and real kinetic motion of the centroids, the overall kinetic energy is not fully available when producing a subthreshold particle.

More details on microscopic models will be discussed in these reports (see chapter "Comparison on Transport Code"), here we wanted only to outline the ingredients and the ambiguities present in the models which should be taken into account when comparing to data. In the next sections we will discuss some relevant features of data and comparison to models. Indeed, since so far no experimental observable has been identified to be directly related to the EOS probes of the different stages of the reaction are necessary to achieve a complete picture of the reaction dynamics and to gather information about the EOS of nuclear matter far from stability. Energetic particles like protons, neutrons pions and gammas were originally proposed to characterize the initial stages of the reactions. It is clear that energetic photons can do that since their mean free path in nuclear matter is very long, thus once they are produced, they are not scattered again. Similarly it is for kaons. We have to cite an early experiment at Ganil at 94 A·MeV where kaons were detected [**18**Julien91]. Since then no further data at that energy regime has been discussed, but we believe we have nowadays very performing detectors which could study kaons produced in heavy ion collisions at around 100 A·MeV. The reasons for using kaons will be more clear after discussing nucleons, pions and hard photons.

SUBTHRESHOLD PION PRODUCTION

Pions (and nucleons), at variance with the other probes, after being produced, might interact with nuclear matter again and be scattered and/or reabsorbed. These multiple interactions of pions with the surrounding matter explain the early success of statistical models [**19**aichelin84,**20**Skyam84,**21**Bonasera87]. This is a reason of ambiguity in transport approaches where the pion production is calculated perturbatively, similarly to hard photons, thus in principle the method is not applicable because the dynamics of the pion after being produced should be followed microscopically. What people does is to correct the results with an absorption factor expressed in terms of a pion mean free path and in turn obtain a value for the mean free path for each experimental conditions [**22**Bauer89,**16**Bertsch88,**15**Bonasera94,**14**Cassing90,**23**Badalà93]. This would be of course very nice if all the other conditions of the calculations had been carefully fixed in parallel experimental situations such as photon production at the same beam energy and systems. Unfortunately, this is rarely reported in the literature we are aware of. In this section we would like to review some of the experimental data on pion production at energies ranging from the absolute kinematical threshold to about 100 A·MeV. The literature at higher energies on pion production is very large but outside the scope of this work and it will be discussed in others chapters.

First data on pion production at subthreshold energies (which is the beam energy per particle in the laboratory below twice the pion mass) was obtained by Benenson et al. at LBL above 100 A·MeV [**24**Benenson79] and subsequently at much lower beam energies, ^{16}O+Al,Ni at 25 A·MeV [**25**Young86]. The latter result was somehow surprising because one would estimate a lower threshold for pion production of 50 A·MeV by coupling the relative to the Fermi motion in first chance NN collisions. In the work of Benenson et al. the ratio of π^+/π^-, that are reported in Fig.4, was measured and was successfully explained in terms of a statistical model which invoked the ratios of the absorption cross sections and a shift due to the Coulomb difference of the two separated and united nuclei divided by the temperature (see full line in Fig.4) [**21**Bonasera87].

A collection of available data was analyzed in terms of probability of elementary NN collisions folded with the number of possible collisions in a nucleus nucleus interaction. This gave a scaling approximation similar to the one reported for photon production and it is displayed in Fig. 5 [**26**KwatoNjock88,**27**Metag88]. This scaling is quite convincing and it shows that at least the gross features could be understood in terms of single NN collisions. However, results like the ratios discussed above and other features we will discuss below hint that when we are very close to the kinematical threshold of the process the naïve model of incoherent NN collisions does not work.

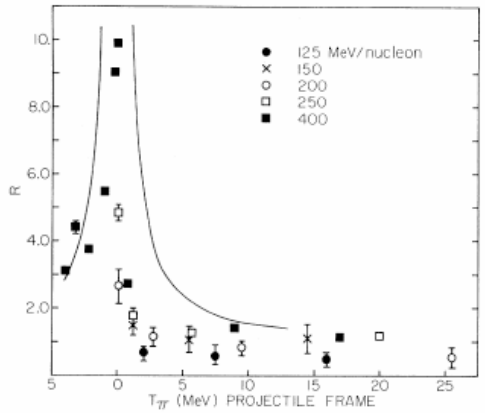

Fig. 4 – Ratio, R of π^- to π^+ cross section in Ne + NaF at different incident energies as a function of the pion energy in the projectile frame. The solid curve shows the Coulomb energy as described in the text [**24**Benenson79].

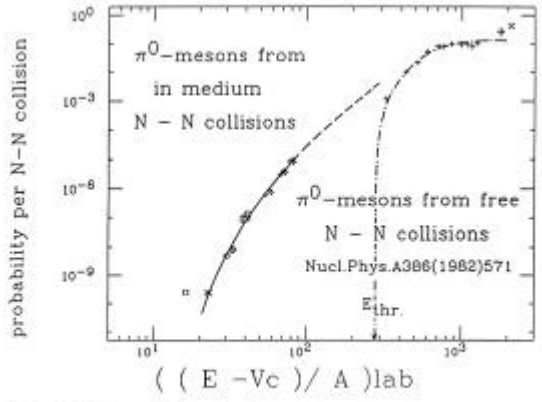

Fig. 5 - Emission probability of neutral pions for in medium nucleon-nucleon collisions as a function of the incident energy per nucleon. Vc is the Coulomb barrier. [**14**Cassing90]

To enter more in detail into the microscopic calculations and their weak and strong points we briefly recall how pion production is simulated in kinetic models. This is very similar to photon production as discussed below i.e., for each elementary NN collision, the production probability is calculated perturbatively. This means, similarly to photons, that for each elementary collision a pion of a given charge (charge conservation enforced) and energy is produced. The emission angles are randomly chosen and the final momenta of the nucleons are calculated to conserve total energy and momenta in the collision. To increase statistics one could choose many times the random emission angles of the pions and average over those emission angles. The obtained probability is multiplied by the Pauli blocking factors (1-f)·(1-f) for each chosen emission angles of the pion (and averaged over the different emission angles). This is exactly the same as for photons production as will be discussed in the next section. This approach has been used by many authors [**16**Bertsh88,**15**Bonasera94,**14**Cassing90] but one different idea was proposed by Bauer [**22**Bauer89]. He assumes that the pion is produced through a Δ resonance which does not decay during the dynamical evolution. In fact, being in a different baryonic state than the nucleons the Δ does not see the Pauli blocking. This is an interesting idea which, maybe, should be pursued more deeply and we will try to give some reasons why. For instance in dense stars one might ask what happens to nuclear matter when it is compressed (essentially at zero temperature). When increasing the density, the star assumed for simplicity to be composed of nucleons only, will increase its Fermi energy. At some density it might be more convenient to produce a Δ baryon which has a larger mass than a nucleon but does not see a strong Pauli blocking i.e. does not have a large Fermi energy. Thus in the compression we might have a mixed state of nucleons and Δ where the latter cannot decay because of the Pauli principle. Of course at even higher densities strange particles or even a quark gluon plasma might be energetically favored. The crucial point for this scenario is to get some information on the mean field seen by the Δ and on the EOS for nucleons. In fact, if the Δ see a strong repulsive mean field, their formation will not be favored and the process discussed above will be unphysical. Gathering some information about the properties of the mean field seen by the Δ at moderate densities and temperatures could be possible through a careful experimental and theoretical analysis of pion and photon production in the nucleus-nucleus collisions. This would call for a second campaign of coincidence experiments with more performing detectors to study the Δ propagation in medium supported by a deep theoretical analysis with more recent and refined models which are now available. Since in the world there are many laboratories able to deliver beams of high quality at the energies of interest and there are very good and performing detectors which with small modifications could be suitable to study the type of physics discussed here, there is no need for large financial efforts and to leave the field not fully explored would be a real

pity. But in order to disentangle between the main features we have understood so far and the questions still not answered we should go in more details into the results we have obtained.

In terms of microscopic models the first ingredient to be considered is the Fermi momentum distribution. In preliminary works the Fermi distribution was given 'by hand' using the Fermi gas model i.e. for each local density a Fermi momentum is calculated and the particles (usually test particles in a Boltzmann transport equation) are randomly distributed as a step function with the given Fermi momentum. Thus the initial distribution was usually not obtained from self consistent ground state calculations such as Hartree-Fock method. This approach lacks of course of self consistency and the high momentum tail of the distribution [**16**Bertsh88,**15**Bonasera94,**14**Cassing90]. More recent approaches such as Fermionic Molecular Dynamics (FMD) [**28**Feldmaier00], Antisymmetrized Molecular Dynamics (AMD) [**29**Ono92], Constrained Molecular Dynamics (CoMD) [**30**Papa01] and more recent Vlasov approach (**31**Lacroix98,**32**Bonasera01ArXi] calculate in a self consistent way the ground state which could be used for the time evolution of the collisions. However, detailed calculations for pion production within the framework of those more refined models are not available to our knowledge.

In the old calculations a large dependence of the pion production on the Fermi momenta was observed. We notice in passing that in the ground state of the nuclei not obtained self consistently one could change the Fermi energy by modifying slightly the surface term or the momentum dependent part of the potential (or some parameters of the Gaussian or delta test particles) in order to have always the same binding energy of the nuclei. Changing the Fermi distribution will change the pions distributions of order of magnitude [**15**Bonasera94]. Even the choice of initially distributing the test particle in momentum space according to some data obtained in electron scattering experiments is ambiguous [**14**Cassing90]. In fact, in that case, Pauli blocking at the surface is not adequately taken into account because of the semiclassical nature of the approaches. As a result within the same model one could obtain particles production even in the ground state because the final momenta of the nucleons initially located in the high momentum part of the distribution are not Pauli blocked unless they are located inside the nucleus both in coordinate and momentum space. This kind of ambiguity did not let us solve the question if the energetic particles are produced in incoherent NN encounters or not. More recent data on proton production as function of the number of participant nucleons [**13**Sapienza01] clearly demonstrates that more cooperative processes have to be invoked when detecting protons whose energies are close to the NN kinematical limit. Similar exclusive data at the energies of interest here and for pion production is not available to our knowledge. This kind of data would, of course, provide more precise information on the type of mechanism responsible for pion and more general particles production near the kinematical threshold. Furthermore they will give a more stringent test to the more refined models available nowadays.

Another ingredient of the calculations is the collision term. Most calculations include a two body collision term which takes into account in a semiclassical way the effect of the Pauli blocking. However, when the density and temperature of the system increase Pauli blocking relaxes and the dilute gas approximation which is the basis of the Boltzmann collision term is no longer valid. Attempts have been done to include the effects of three body collisions [**33**Kodama84,**34**Bonasera92,**35**Danielewicz92) to calculate not only particles production and collective effects [**15**Bonasera94] but also more complex particles production [**35**Danielewicz92]. We would like to notice at this point that there is a different way the 3-body collision term is treated in [**33**Kodama84,**35**Danielewicz92] and in [**34**Bonasera92]. In fact in [**33**Kodama84,**35**Danielewicz92] a 3-body collision can happen if the particles did not undergo a 2-body collision while in [**34**Bonasera92] the probabilities for 2 and 3 body collisions are calculated independently. This latter assumption leads to a decrease of the particles mean free path while the previous does not necessarily. The two approaches give different values for physical observable such as collective flow under fixed conditions for the other parameters, i.e. same elementary NN cross section and similar momentum independent mean field. For momentum dependent mean field the number of collisions are reduced because the strong repulsive effect of

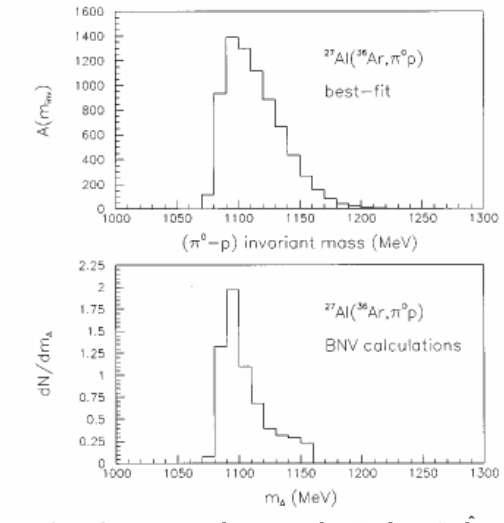

Fig. 6 – Comparison between the "indirect"-channel (π^0-p) invariant-mass distribution A(m_{inv}) (upper panel), extracted from a best fit procedure, and Δ mass distribution (lower panel) predicted by the BNV theoretical calculation for the same system at the same bombarding energy [**37**Badalà96]

the mean field when the particles collide and change their momenta. This will be discussed more in detail below for particles production where the momentum dependent part is even more important. As far as resolving the ambiguity to treat the 3-body collisions term microscopically, a test was proposed in [**34**Bonasera92] for a Maxwell and a Fermionic gas in equilibrium at temperature T where the number of 2 and 3 body collisions could be estimated analytically. A similar strategy should be pursued in order to eliminate differences among numerical codes that in principle solve the same equation. Neverthless when 3 body collisions are included energetic particles are produced with higher probability as compared to the 2 body case and with higher energies [**15**Bonasera94].

Another important physical ingredient is the nuclear mean field. Many calculations have shown a modest sensitivity to the compressibility of the EOS for pion and photon production. This has been explored especially for momentum independent interactions. Of course it is well known that the mean field is momentum dependent (Fig.2) thus models should take into account this feature also for particles production. As we introduced above when the momenta of two (or three) colliding nucleons change because of the scattering, the field changes as well because of its momentum dependence. What one does in practical calculations is to modify the momenta of the particles in such a way that the total energy is conserved. If this is not possible the collision is rejected. This generally results in a reduced number of NN collisions and possibly in a transparency effect of the nucleus-nucleus collision as compared to calculations with momentum independent forces. The role of the momentum dependent force should be further investigated when a particle, a pion or a photon is produced. In such a case the final momenta of the nucleons are further reduced because some energy and momentum is carried away from the produced particles. Thus, on top of the Pauli blocking effect one should consider the effect of the momentum dependent mean field which being usually repulsive will result in a need for more energy to produce a particle and in turn to a reduction of its formation probability. No microscopic models with momentum dependent forces which calculate subthreshold particles production are available to our knowledge. Some exist at higher energies where the calculations are non perturbative [**36**Aichelin85] and a sensitivity to the EOS is demonstrated. Even in the perturbative regime calculations should be feasible nowadays with the more performing computers.

For the particular case of pion production, if the process occurs through Δ formation and if the Δ cannot decay because of the Pauli principle until it is in vacuum (or in a low density and high temperature region) one could try to study the properties of the mean field seen by the Δ. Some experimental data on Δ production in nucleus-nucleus collisions at energy below 100 A·MeV has been discussed in [**37**Badalà96,**38**Badalà98] and investigated in BNV calculations (see Fig.6). The data shows that the Δ width is reduced from its free value to about 25-50 MeV. Naively this would indicate that the delta lifetime in the matter increased to about 10 fm/c which could be a sufficient time to say that the delta does not decay before the nuclei disassemble. On the other hand the width of the resonance is roughly reproduced in the BNV calculation as due to the folding of the delta width in vacuum and energy conservation (or Pauli blocking) which blocks the higher momentum part of the pions distribution. The model has the features discussed above, i.e. momentum independent mean field, Fermi gas approximation for the initial distribution and two body collisions only. A more refined approach and more data for other systems at different energies would be greatly helpful to study the dynamics of the Δ in nuclear matter moderately excited.

We notice in passing that the model calculations are also sensitive to 'hidden' parameters of the numerical solutions. These might be the width of the Gaussians if one uses Gaussians test particles, or the cell sizes if one uses delta test particles or any other parameters that one might use. A comparison among codes is discussed in the chapter "Comparison on Transport Code". Those differences among numerical codes should be resolved before any physical conclusion can be obtained.

HARD PHOTON PRODUCTION

The spectrum of photons emitted in heavy ion collisions at intermediate energies carries a lot of information on the system evolution from the very early stages of the nucleus-nucleus collisions to the latest phase at the end of the de-excitation stage after particle emission. We will show that hard photons are particularly appealing probes since they do not interact again with the surrounding nuclear matter after the production and therefore could also provide information on the chronology of the nuclear dynamics at various stages of the reaction. A typical spectrum of photons emitted in heavy ion collisions at intermediate energies is reported in Fig. 7 for the reaction ^{36}Ar+^{98}Mo at 37 A·MeV [**39**Piattelli96]. As a first rough classification we can divided the spectrum in three main regions with increasing energies:

- in the energy range from some hundreds of eV to several MeV (E_γ<10 MeV) the spectrum is dominated by the statistical emission from excited nuclei occurring at the end of the de-excitation process.
- in the energy range between roughly 10 MeV and 20 MeV a bump due to the γ decay of the Giant Dipole Resonance (GDR) , which is a major isovector collective mode in nuclei can be observed [**40**SNO86,**41**GAR92]. The γ decay of the GDR has been extensively investigated also in hot nuclei in order to gather information on the maximum temperature that a nucleus can hold. [**42**LEF94]. This subject is covered in the chapter of this review "GDR Quencing".
- in the energy range beyond 30 MeV the spectrum is characterized by a large inverse slope parameter which increase with increasing energy and with a yield which, for a given incident energy per nucleon, increases with the size of the colliding nuclei. These high energy gamma rays (E_γ> 30 MeV) are the so called hard photons, and are the subject of this part of our review and their production has been deeply investigated. The main results will be reported in the following with the current understanding of the hard photon emission and open problems which still need further investigations.

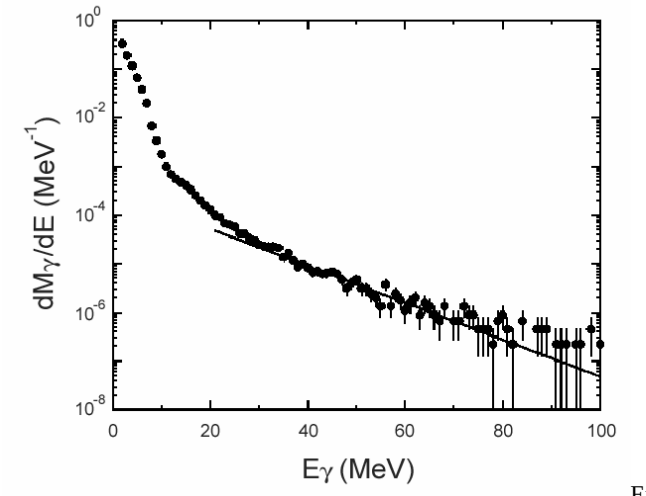

Fig. 7 – Gamma multiplicity spectrum for incomplete fusion reactions in the ^{36}Ar + ^{98}Mo system at 37A·MeV. The continuous line indicates the exponential fit of the hard component (E_γ > 35 MeV). [**39**Piattelli96]

The first experimental observation of an unexpected hard component in the photon spectrum emitted in nucleus-nucleus collisions was found in the ^{12}C+^{12}C at 84 A·MeV reaction. It was investigated aiming at the study of subthreshold π^0, which decays by the emission of two energetic photons, there the hard photons represented a background [**43**NO84]. The analysis of these first data [**44**GRO85,86] produced a lot of interest from both the experimental and theoretical point of view. Indeed, in spite of the very low hard photon cross section several (inclusive) experiments followed with various projectile-target combinations on a rather broad energy range between 10 A·MeV [**45**Gan94] and 124 A·MeV [**46**CLA89]. Inclusive experiments yield information about hard photon cross sections, inverse slope parameters, angular distributions and source velocities. From a theoretical point of view, the question about the origin, i.e. the production mechanisms, of the hard photon emission was also faced and the proposed solution can be summarized in terms of the following main hypotheses:

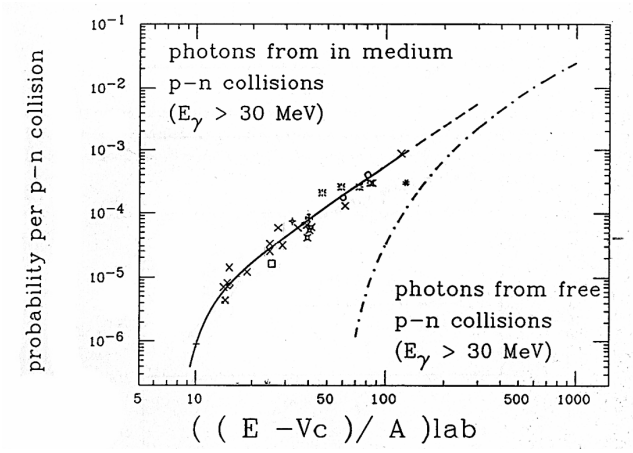

Fig. 8 – Emission probability for photons with E_γ>30 MeV per in-medium nucleon-nucleon collisions as a function of the incident energy per nucleon. Vc is the Coulomb barrier [**27**Metag88]

- nucleus-nucleus collective bremsstrahlung [**47**VA84,**48**KO85,**49**Nak87] where the photons are emitted as a consequence of the coherent deceleration of the electric field of the two colliding nuclei. The photon yield strongly increases with increasing energy and the spectrum slope depends on the deceleration time;
- incoherent bremsstrahlung as a consequence of nucleon-nucleon, in particular n-p, collisions occurring in the interaction region in the first stages of the reaction [**50**BAU86,**51**REM86] as radiation due to the proton deceleration. Several prescriptions have been used for the np→npγ cross section such as the semi-classical one [**52**Jackson], the neutral scalar meson exchange model etc etc [**53**Cassing86,**54**Nak89).

- statistical emission either from a compound-like emission [**55**Hermann88] or from a "fireball" like system [**56**NI85], where the spectrum slope should reflect the temperature of the emitting source;
- cooperative effects where several nucleons group together into virtual clusters which provide the extra energy for the hard photon production [**57**SHY86].

The inclusive data systematics gave evidence of a source velocity close to half the beam velocities and an angular emission pattern consistent with an isotropic plus a dipole like emission in the source reference frame [**14**Cas90]. These results seem to be consistent with the n-p bremsstrahulng mechanism as a dominant process in the hard photon emission in heavy ion collision at intermediate energy. The hard photon emission however exhibits a much larger yield than expected from free n-p collisions, this difference is strongly increasing with decreasing beam energy (Fig.8). For this reason the hard photons are considered as "subthreshold particle" using the same definition that applies for meson when they are produced at incident per nucleon lower than the energy threshold for nucleon-nucleon collision. Moreover, some results have been rather well reproduced by a statistical approach, i.e. the experiments ^{92}Mo + ^{92}Mo at 19 A·MeV [**55**HE88] and N+(C, Zn, Pb) at 20, 30 and 40 A·MeV [**58**STE86], while the hard photon angular distribution in asymmetric systems [**59**BRE89,**60**TAM88] is well consistent with a source velocity close to the half beam velocity with the presence of a dipole component rather than to the compound nucleus velocity. Moreover, the unique result indicating evidences of coherent bremsstrahlung [**61**Alamanos86] was not confirmed. Anyway the expected yield for collective nucleus-nucleus bremsstrahlung [**48**KO85] is much lower than the observed ones.

Beside the understanding of the production mechanism, the study of the hard photon emission allows to use them as probes of the nuclear matter. In particular, due to the nature of the electromagnetic radiation, this probe can carry unperturbed information on the nuclear matter at the moment of their production and are not affected by subsequent stages of the reaction. Information on nuclear dynamics, on the contribution of the mean field and two body collisions in dissipative heavy ion collision and a time scale for multifragmentation have been deduced by detailed investigation of the hard photon emission in heavy collisions at intermediate energy and the main results are reviewed in the following**.**

Hard photons are expected to be a good probe up 90 A·MeV since at higher incident energies the contributions of the π^0 decay cannot be neglected (see Fig. 5 and Fig. 8). Dynamical calculations indicate that the cross section dependence on the incident energy per nucleon (E_γ> 50 MeV) [**50**BAU86] are consistent with at most 10% of the observed cross section due to nucleus-nucleus bremsstrahlung, while the dominant part of the total yield is due to

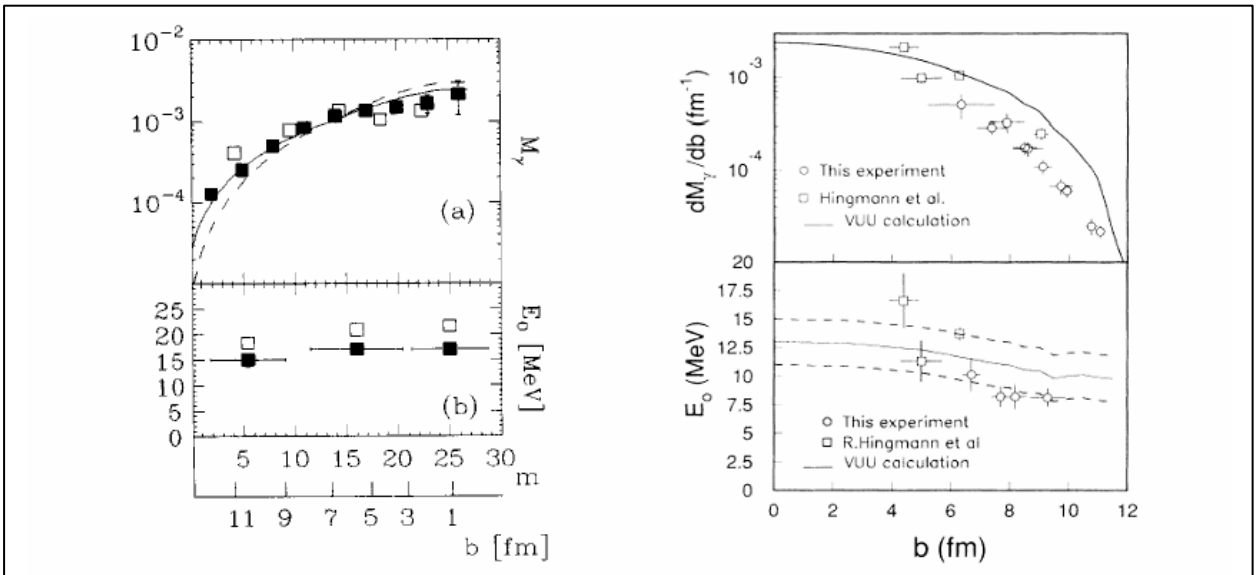

Fig. – 9 – Gamma ray multiplicity for E_γ>40 MeV (left top panel) and for E_γ>25 MeV (right top panel) and inverse slope parameters as a function of the centrality for the reaction Xe+ Au at 44 A·MeV [67Migneco93] (solid squares in the left panels) and for the reaction Ar+Gd at 44 A·MeV open symbols in the right panels [66Riess92]. In the left panels for comparison BNV calculations are reported (open symbols) while the continuous line is calculated assuming M_γ proportional to the surface of the overlap area and the dashed line is calculated assuming M_γ proportional to the volume of overlap area . In the right panels VUU simulations are reported (full lines, dashed curves are the uncertainties)

first chance n-p collisions. It is important to note, however that inclusive data are also consistent with n-p bremsstrahlung in a nuclear fireball.

In order to disentangle between the different hypotheses concerning the origin of the hard photon emission and to get a deeper insight on the phenomenon, exclusive measurements were necessary. A first group of measurements faced the issue of the impact parameter dependence of the hard photon production. The first experiments indicated that the hard photon multiplicity increases with increasing reaction centrality as expected from various models and the slope slightly decreases with increasing impact parameter [**58**STE86,**62**HIN87,**26**KWA89,**63**REP92].

Results from calculations indicate that the hard photon multiplicity scales with the volume of the interaction zone, which increases with increasing centrality, for the emission from a fireball [**56**NIF85], while in dynamical calculations like BUU [**50**BAU86], where hard photons (E_γ>50 MeV) are mostly emitted as a consequence of first n-p collisions, a hard photon multiplicity dependence on the overlapping circles is found consistently with emission in the first stages of the reaction [**50**BAU86]. Moreover, in dynamical calculations, the decreasing of the slope with increasing impact parameter is interpreted as due to the fact that nucleons with softer momentum are mostly located at the nuclear surface.

A very good review of the hard photon production is included in the reference [**14**CAS90] where the possibility of exploiting energetic particles as probes of the first stages of the reaction is deeply investigated.

However, due to the low production cross section, the quality of the exclusive experiments and data was strongly boosted by the high efficiency of two multidetector apparata for hard photons, namely MEDEA (87% efficiency) where hard photons and light charged particle can be detected simultaneously [**1**Migneco92] and TAPS [**5**Martinez97]. In particular, the dependence of the hard photon multiplicity M_γ on the impact parameter b was investigated quantitatively. In the models based on n-p bremsstrahlung, the hard photon multiplicity scales with the number of n-p collisions and therefore with the size of the interaction zone $M_\gamma(b) = P_\gamma \cdot N_{np}(b) \propto P_\gamma \cdot A_{part}(b)$ where P_γ is the probability of emitting an hard photon in a single n-p collision (p-p collisions are not considered since they provide a much smaller contribution ≤10%) at a given incident energy for heavy ion reaction and is usually extracted from the inclusive data (see **27**ME88 for systematics) within the approximation that P_γ in nuclei only depend on the incident energy per nucleon. Several experiments [**64**RIE92,**65**MIG93,**66**MAR94] were run and compared with the results of dynamical model based on transport equation to simulated the nucleus-nucleus collisions where the hard photon production is treated in a perturbative way. In Fig.9 the measured and calculated M_γ and inverse slope parameters as a function of the estimated impact parameters are reported for two different reactions measured with two different apparata. In general, a rather good quality agreement between the measured and calculate hard photon multiplicity for several reactions is observed. Moreover, a dependence closer to the surface of the overlapping circles rather than to the volume was found in the reaction $^{129}Xe+^{197}Au$ at 44 A·MeV (see Fig 9 top left panel) where a good agreement with BNV calculation was found [**65**MIG93]. These results provide a further support for the models based on n-p bremsstrahlung. Similar information was gathered from inclusive data with varying the size of the colliding nuclei. Anyway, this large set of data although consistent with BUU calculations**,** cannot rule out a fireball scenario especially at the higher incident energies. Eventually, these experimental data provide a measurement of the spatial origin of the hard photons from the interaction zone. However, it is important to underline that, the fact the hard photon multiplicity scales linearly with the participant region, not necessarily imply that a fireball is formed as an independent source, but, especially at the lower incident energy regime around the Fermi energy, rather provides a snapshot of the interaction zone in the early stage of the reaction. For this reason the hard photon multiplicity can also be used as a quantitative measure of the impact parameter in heavy ion collisions.

A deeper insight on the hard photon production mechanisms was attempted by looking at hard photon particle correlations and hard two photon correlations. In calculation where the hard photons mainly arise from first chance n-p collisions, if the photon and proton energy are high enough an anticorrelation between energetic proton emission is expected due to the kinematical limit imposed on the total proton and gamma-ray energy when the observed proton is the bremsstrahlung generating proton. In the reaction $^{14}N+Zn$ at 40 A·MeV the gamma-ray proton coincident ratio was found to be independent of proton energy for E_γ>20 MeV, thus suggesting that the high energy photon production, for E_γ > 20 MeV, may arise in part from n-p bremsstrahlumg in a later stage of the collision [**67**LAM88]. On the other hand, high statistics data on the reaction $^{40}Ar+^{51}V$ at 44 A·MeV [**68**SA94]show that while hard photons with E_γ>25 MeV exhibit a slight anticorrelation constant with increasing energy, the very energetic photons, namely with E_γ> 70 MeV exhibit a much stronger anticorrelation increasing with increasing proton energy as expected in a first chance n-p bremsstrahlung scenario. This result**,** which confirms the expectation of the dynamical models (see **14**CAS90), provide an experimental evidence of the hypothesis that the very energetic photons are mostly produced in the early stage of the reactions. This unambiguous signature qualifies high energy

photons, and protons, as probes of the momentum and energy distributions of the nucleons in the early stages of heavy ion collisions**.**

The hard two-photon correlations was investigated in different systems and the results reported in ref.[**69**BAD95,**70**BAR96] also supports the idea that hard photons originate from an early stage of the reaction. A contribution from a second, less energetic, photon source emitted in a later phase of the reaction was put in evidence in several reaction at various incident energy beam. The feature of this so called "thermalized" hard photon component and its consistency with statistical and dynamical model calculation are discussed in the next paragraph.

In heavy ion collisions at intermediate energy, especially around the Fermi energy, the nuclear dynamics is governed by the interplay between one and two body dissipation, namely between the mean field and nucleon-nucleon collisions. At energy around and above the Fermi energy (about 35 MeV) the role of nucleon-nucleon collisions increases with increasing incident energy due to a minor contribution of the Pauli blocking, which inhibits the nucleon-nucleon collisions at low energy. Two different experiments addressed the problem of one and two body dissipation mechanism at intermediate energy via the study of the hard photon emission in peripheral and central reaction respectively.

Hard photons were measured in coincidence with projectile-like fragments in the reaction ^{36}Ar+^{159}Tb at 44 A·MeV in the peripheral events [**71**VAN96]. The hard photon multiplicity, which scales with the number of n-p collisions as discussed above and therefore represent a measure of the two body dissipation, was measured as a function of the mass of the primary projectile-like mass and was found to increases linearly with the transferred mass, putting in evidence the importance of two body collisions. Moreover, the multiplicity value depends on the direction of transfer, indeed more collisions are needed to transfer mass from the heavier target then vice versa, this effect is understood in terms of the action of the mean field that favors the nucleon transfer from the lighter to the heavier partner of the collision. A complementary study for central collisions leading to incomplete fusion residues is reported in ref. [**72**PIA98]. In this case, hard photons (E_γ > 35 MeV) were measured in coincidence with heavy residues emitted in the reactions ^{36}Ar+^{90}Zr at 27 A·MeV and ^{36}Ar+^{98}Mo at 37 A·MeV. In this incident energy regime central and semi-central collisions lead to incomplete fusion and this process is usually described by the Viola systematics which shows a decrease of the momentum transfer as a function of the incident increasing energy [**73**VIO82]. In the two ^{36}Ar induced reactions cited above the ratio between residue velocities and the center of mass velocities (v_r/v_{cm})was measured as a function of the reduced impact parameter (b/b_{max}) given by the hard photon multiplicity. A strong correlation is found between v_r/v_{cm} and b/b_{max} and more remarkably the data coincide for both incident energies investigated indicating that the fraction of linear momentum transfer for events giving rise to a residue depends only on impact parameter and not on bombarding energy thus demonstrating the role of two-body collisions in the transfer process leading to the production of highly excited nuclei. In conclusion, the hard photon detection has played an important role in elucidating the interplay between mean field and nucleon-nucleon collisions around the Fermi energy both in peripheral and central collision, leading respectively to PLF fragments and Heavy Residues.

"Thermal" hard photons

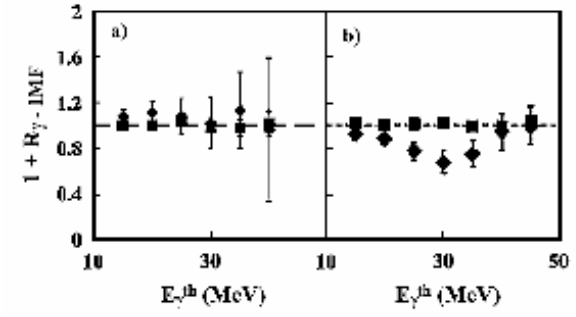

Fig.- 10 - Experimental photon-IMF correlation factors versus the threshold E_γ for IMF's in two velocity windows: diamonds IMF velocities near the c.o.m. velocity and squares for IMF velocities higher than the c.o.m. velocity. Data are shown for the Ni+Au reaction at 30 A·MeV (a) and 45 A·MeV (b), for central collisions.

Hard photons (E_γ>30 MeV) were measured in the reactions induced by an ^{36}Ar beam at 95 A·MeV on ^{197}Au and ^{12}C. *It is important to note that in this case the incident energy per nucleon is well above the nucleon-nucleon free threshold for the production of photons with E_g>30 MeV.* The bulk of data analyzed in these experiments indicates that while the very energetic photons originate from the first phase of the reaction, as proved in [**67**SAP94], the bulk of photons (E_γ>30 MeV) is produced over a longer time span and could probe the phase that leads to the thermalization of the fireball if it is formed in the reaction [**74**SCHU94]. From an experimental point view the very good statistics achieved in hard photon measurements in heavy ion collisions at intermediate with the MEDEA **[1]** and TAPS **[5]** detectors allows to put in evidence that a good description of hard

photon spectra is obtained with the superposition of two component with different slopes and yields**.** However, we would like to notice that the change in slope of the photon yield could be also affected by the $1/E_\gamma$? factor which enters the elementary np->npγ bremsstrahlung probability [15Bonasera94]. Moreover, hard two-photon interferometry measurements in the reactions ^{86}Kr+^{nat}Ni at 60 A·MeV and ^{181}Ta+^{197}Au at 39.5 A·MeV are well described within the hypothesis of two different sources [**75**MARQ95]. The softer component has been associated to photon emission in a later stage of the reaction. In BUU calculations, aside the hard photons produced by the bremsstrahlung emitted in n-p collisions, that occur during the compression phase at the early stages of the reaction ("direct" photons) and constitute the dominant contribution, "thermal" hard photons are also emitted in a later stage from a thermalized source during the resilience of the system after the expansion phase from less energetic n-p collisions. Experimentally, inclusive and exclusive photon spectra consistent with a "thermal" and "direct" component were measured in the reactions ^{86}Kr + ^{nat}Ni at 60 A·MeV, ^{181}Ta + ^{197}Au at 39.5 A·MeV, ^{208}Pb + ^{197}Au at 29.5 A·MeV [**76**MART95] and in the reactions ^{36}Ar + (^{197}Au, ^{107}Ag, ^{58}Ni and ^{12}C) at 60 A·MeV [**77**DEN2001] and in the reactions ^{58}Ni + (^{27}Al, ^{58}Ni and ^{197}Au) at 30 A·MeV **[78**ALBA99**]** and ^{58}Ni + ^{197}Au at 45 A·MeV a [**79**ALB01-05]. An appealing aspect of thermal photons is that their emission signals that a big piece of nuclear matter still exists at the end of the dynamical evolution of the collision and their slopes can be related to the temperature of such a system. This can be exploited to get information on other processes using thermal photons as a probe. For instance, the nuclear caloric curve has been investigated using thermal photons as a new 'thermometer' for hot nuclear matter [**80**Den02].

Also, thermal photons have been used as a 'clock' to deduce the timescale of intermediate mass fragment emission. Studying the thermal photon-IMF correlations, an anticorrelation signal with IMF's in the nucleus-nucleus centre of mass velocity region has been observed in central Ni+Au collisions at 45A MeV, while the same has not been seen in the data for the same system at 30A MeV (fig.10). This indicates a transition to prompt IMF emission, namely before the emission time associated to thermal photons, to show up around 45A MeV. Moreover, stochastic mean field simulations performed for these two reactions are consistent with the data since at 30 A·MeV for most of the events the system, after the initial compression and expansion, the recompounds leading to the formation of an heavy excited system with Z around to 80. On the other hand, at 45 A·MeV a dominant role of a prompt IMF formation is observed [**79**ALB04-05].

Deep sub-threshold hard photon emission

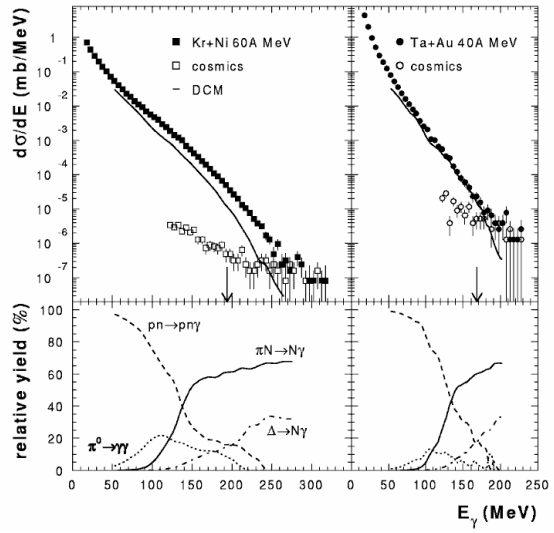

Fig.-11- Mesured photon spectrum (full symbols) in the reactions ^{86}Kr + ^{nat}Ni at 60 A·MeV left panel and ^{181}Ta + ^{197}Au at 40 A·MeV right panel after the subtraction of the cosmic-ray contribution (open symbols). The solid line represents the calculations. In the lower part the calculated spectrum is decomposed into fractions corresponding to the following mechanisms: pn ® png, p**N**® **N**g, p° ® g g, D® Ng **[81GUD96]**

Deep sub-threshold particles, with respect to the kinematical limit expected for nucleon-nucleon collision including the boost due to the Fermi motion, are observed on a broad range of incident energies addressing the question of which mechanism allows to concentrate a relevant fraction of the total available energy in the production of a single energetic or massive "particle". Several hypotheses have considered such as nucleon off-shell effects, three-body collisions, dynamical fluctuations or multi-step processes involving pion and delta.

High statistics hard photon data exhibit the presence of hard photons with energy well above the kinematical limit for nucleon-nucleon collisions. In the reactions ^{86}Kr + ^{nat}Ni at 60 A·MeV and ^{181}Ta + ^{197}Au at 40 A·MeV [**81**GUD96].hard photon spectrum, with energy extending up to 5 times the beam energy for nucleon, were measured. The data were compared with a cascade model which takes into account several channels (see Fig. 11) including the radiative channel π+N->N+γ. The calculations are in good agreement with the data for the reaction ^{181}Ta + ^{197}Au at 40 A·MeV, while undershoot the data of the reaction ^{86}Kr + ^{nat}Ni at 60 A·MeV both concerning the highest energy component of the photon spectrum and slope and yield of the π^0 energy spectrum.

In summary, theoretical calculations, in spite of the many hypotheses proposed, are not satisfactory in explaining deep subthreshold data and a more detailed comparison between data and models is desirable.

ENERGETIC LIGHT PARTICLE EMISSION

The energetic particle emission, that occurs in the first phase of the reaction, is of particular interest in the intermediate energy domain where the interplay between one and two body forces strongly affects the reaction dynamics. Together with pions and hard photons, energetic nucleons are a powerful probe to get information on the first compressed nuclear phase and on the reaction dynamics because their emission drives the system towards an expanded and more thermalized stage or a multi-fragmentation stage. Moreover the knowledge of the energetic particles multiplicity and of the energy dissipated in the first reaction phase is of particular interest for the understanding of the role of the isospin degree of freedom in nuclear reactions and in the EOS for asymmetric nuclear matter.

Energy spectra of light particles (p, d, t, He) have been measured for a large variety of reactions in a wide range

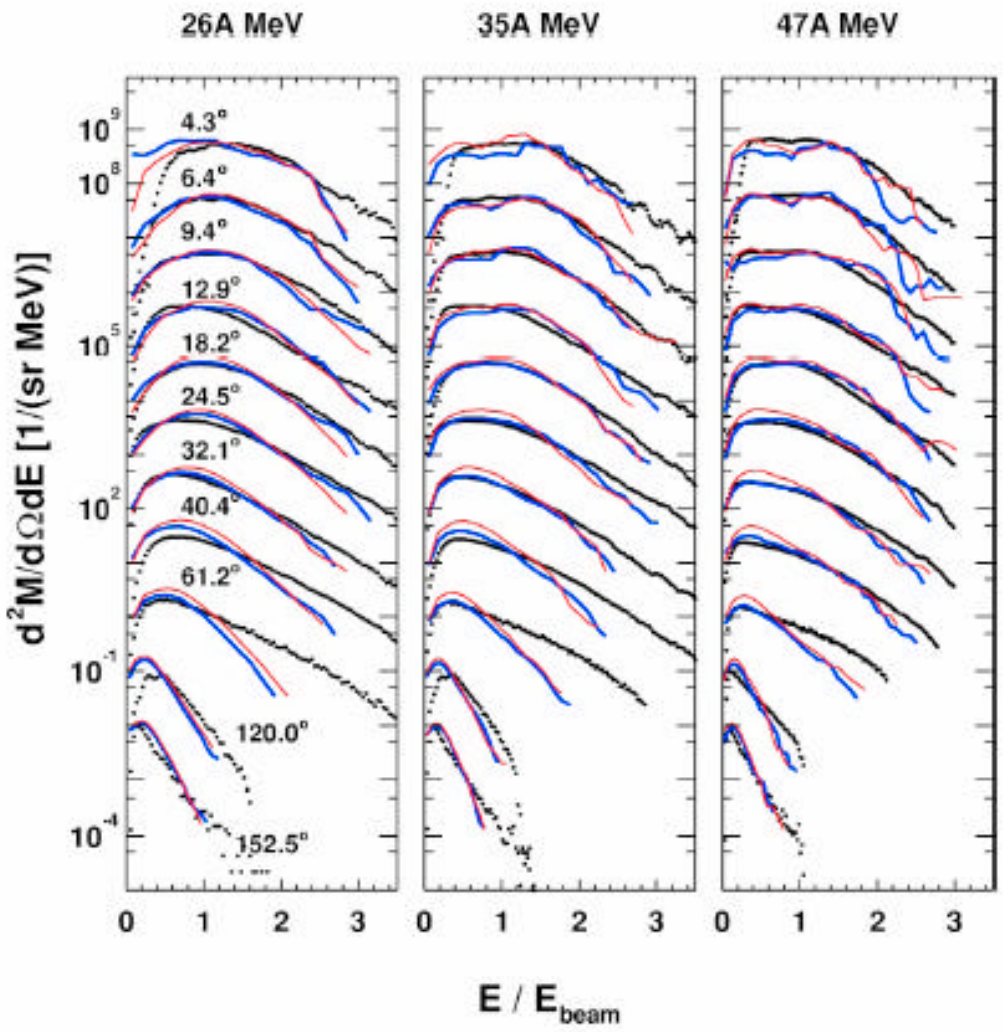

FIG 12. Proton energy spectra for violent collisions in ^{64}Zn + ^{92}Mo reactions at different incident energies (indicated on top) and different detection polar angles. (indicated in the left column) are reported. Experimental data results are shown by dots. Thick and thin solid lines refer to AMD-V simulation results for soft and stiff EOS with different prescription of in medium cross section [**3**Wada04].

of incident energies with apparatus covering the whole angular range. In Fig. 12 are reported the experimental proton energy spectra (dots) for the ^{64}Zn + ^{92}Mo collected at different incident energy and detection polar angles measured with the NIMROD apparatus [**3**Wada04]. The common analysis used to study the light particle emission mechanisms is the simultaneous fit (in energy and in angle) of these spectra assuming isotropic emission from sources with a Maxwellian spectrum in its center of mass. Such analysis performed on energy spectra, collected in inclusive [**82**Awes81,**83**Awes82,**84**Westfall84,**85**Jacak87,**86**Fukuda84] and as function of the centrality [**87**alba94,**88**Santonocito02,**89**Wada89,**90**Hasselquist85] shows that the procedure is able to give a qualitative characterization of the light particles emission process.

The source velocities (v_s), the inverse slope parameter (T), the multiplicity (M) and the Coulomb emission barrier (E_c) are the fit parameters. A good reproduction of the experimental data, in the whole angular range, is possible only if three sources are taken into account: a projectile-like source (PLF) ($v_s \sim v_{beam}$) that dominate at forward angles, a target-like source (TLF) ($v_s \sim 0$) localized at low energies and an intermediate velocity source (IS) ($v_s \sim v_{beam}/2$) that dominate at high energies and at larger polar angles. The source relative yields depend on the system asymmetry, on the reaction centrality [**88**Santonocito02,**89**Wada89] and incident energy. The values of inverse slope parameter (T) are of the order of 4-6 MeV for TLF and PLF while, for the IS source, T assumes much higher values, depending on the incident reaction energy. The presence of these three sources is clearly evidenced also in the Lorentz invariant differential cross section plots for light particles [**91**Pawloswski00,**88**santonocito02].

Light particles emitted from TLF and PLF sources are interpreted as particles evaporated from equilibrated systems with a statistically predicted Maxwellian spectrum. Such interpretation is strengthened by the analysis at lower bombarding energy and/or excitation energy. The exponential slope T reflects the "apparent temperature" of the emitting systems averaged over the whole de-excitation cascade. Applying correction (statistical models) it is possible to estimate the initial temperatures that are in agreement with the values estimated with other methods [**80**Natowitz02].

Protons and neutrons emitted from a source with half beam velocity (IS), which account for the most energetic part of the spectra at around 90° in the half beam reference frame, are interpreted as emitted in a non-equilibrated phase of the reaction as a consequence of nucleon-nucleon collisions. In ref [**92**Plagnol00] midvelocity emission is already found at 25 A·MeV while the onset of hard photon emission, discussed in the previous paragraph, is found at 10 A·MeV [**45**GAN94]. For the IS protons the origin of the maxwellian spectrum in the half beam reference frame arise not from statistical argument but from the assumption of independent Gaussian distributions, for the three momentum components, of nucleon Fermi momenta with $\sigma^2 = m\,T$ where σ^2 is the Gaussian mean square value, m is the nucleon mass and T the Maxwellian temperature term [**93**Fucks94]. In particular for IS protons the systematic of the extracted slope parameters T can be explained in terms of random composition of the beam velocity with the Fermi momenta of nucleons inside the nucleus (see Fig.13). Deviation from this law, especially at low incident energy, has been explained as due to Pauli blocking effects [**93**Fucks94].

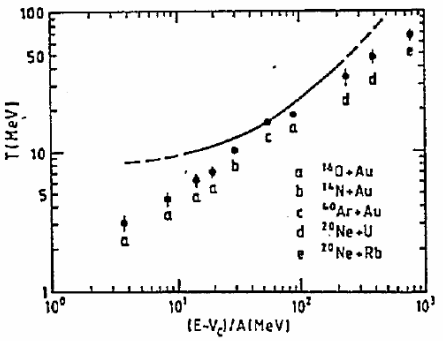

Fig.13- Experimental slope parameters of the IS in proton spectra for various systems as a function of the bombarding energy above the Coulomb barrier V_c. The curve represents the estimate for quasi free nucleon-nucleon scattering [**93**Fucks94]

Analyzing the neutron energy spectra we expect to find the same characteristics with respect to protons (the only difference is the lack of Coulomb repulsion). From the experimental point of view the neutron detection, especially at high energies, is quite difficult and poor experimental data with respect to charged particles are available. In the ^{35}Cl + ^{nat}Ta reaction at 43 A·MeV [**94**Larochelle99] neutron spectra have been measured up to 50 MeV from 60° to 150° polar angles has a function of the PLF excitation energies and preequilibrium neutrons from the IS source have been evidenced. In this work from the Maxwellian fit a IS velocity lower than the half beam velocity for all the PLF excitation energies has been extracted and confirmed by BNV calculations. This trend has been explained as due to the attractive mean field from the target that, the moderately high energy neutrons emitted still feel. In the scenario where preequilibrium neutrons are emitted as a consequence of nucleon-nucleon collisions, if the emitted neutron undergoes to more than one collision a velocity lower than the nucleon-nucleon velocity is expected. Recently, although neutron spectra were measured only up to 25 MeV in the ^{36}Ar+^{58}Ni at 50 A·MeV from 60° to 150°, [**95**Theireault05] they were analyzed as a function of the centrality and the IS velocity was extracted.

The IS velocity is found closer and closer to the nucleon-nucleon center of mass velocity as increasing the centrality. The analysis on proton spectra, presented in the same work but in the ^{58}Ni+^{58}Ni reaction at 52 A·MeV does not show the same trend; the IS velocity is near to the nucleon-nucleon velocity for all the centrality bins. This trend can be explained if the neutrons are emitted both from nucleon-nucleon collisions in the interaction zone in the first stage of the reaction (predominant at central collisions) and/or by a delayed emission that occurs after the neck rupture and enhanced near the heaviest partner of the reaction thus explaining the lower IS velocity at peripheral and semi-central collisions for neutrons. This delayed emission near the quasi-target is enhanced for neutrons with respect to protons due to the lack of the Coulomb repulsion. To confirm this interpretation more simultaneous measurements of protons and neutrons for the same reactions are necessary [**96**ghetti00].

Analysis in terms of Maxwellian source emission applied on light cluster (d, t, He) energy spectra shows a similar scenario. The emission of the most energetic particles from the IS has been explained with a coalescence model where the emission of light clusters is related to the momentum space densities of nucleon in the collision [**86**Fukuda84,**85**jacak87,**97**jacak85,**82**awes81]. The coalescence radius, P_0, is the single free parameter of the model once that proton and neutron energy spectra are known. P_0 is the radius of a sphere in momentum space where the coalescence occurs. Recently the coalescence model has been coupled with dynamical models describing the collision [**91**Pawlowski00,**98**Hagel00,**99**Avdeichikov04] to explain the light complex particles energy spectra. The percentage of particles emitted promptly at intermediate velocity (pre-equilibrium particles) decreases increasing the mass cluster [**91**Pawlowski00]. In ref [**98**Hagel2000] a self consistent coalescence model analysis has been used to determine the size of the system as function of time and follow the evolution of density and temperature during the reaction. Recently, the emission of light cluster (Z≥2) at mid-velocities has been interpreted as emitted from a neck-like structure, formed dynamically during the reaction, joining the quasi-projectile and the quasi-target [**100**Milazzo05 DeFilippo05 and reference therein]. The interest in the study of these light fragments is focused on the understanding of statistical and/or dynamical emission of fragments that can lead the system to the equilibration (see chapter "Neck Dynamics"). Microscopically light clusters formation has been calculated in transport approaches including in-medium effects, which depend on the density and energies deposited in the system [**101**Kuhrts2001]. The agreement of the calculations to data is reasonable.

This well established scenario, in terms of three emitting sources, is a way to mimic the emission of particles dynamically originated during all the reaction time. In particular pre-equilibrium particles are not necessarily emitted from a source well located in time-space. The comparison of experimental data with dynamical model predictions [**12**Coniglione00] and more complex analysis as particle-particle correlations (see chapter "Space Time Characterization I and II") [**102**Ghetti01,**103**verde02], allows to infer a space-time characterization of the emission mechanisms. However, from the experimental point of view, the emitting source parameterization is able to give an estimate of the number of nucleons and of the energy removed at each steps in the reaction [**87**Santonocito02] and to "isolate", putting cuts in the detection angles and energies, energetic particles emitted from the IS (pre-equilibrium particles) for more complex event based analysis [**87**Alba94,**13**Sapienza01].

First measures of the impact parameter dependence of pre-equilibrium particles have been reported in ref [**104**Peter90,**87**alba94,**105**Prindle93] allowing a space characterization of the pre-equilibrium emission. Energetic protons at large polar angles, measured as a function of the impact parameter for reactions with different mass asymmetry at 44 A·MeV [**87**Alba94], show that pre-equilibrium proton multiplicities scale as the size of the overlapping region and from system to system as the number of protons in the collision zone. In particular a better agreement is found with the impact parameter dependence of the overlap surface of the colliding system thus indicating that pre-equilibrium protons are emitted mainly from first NN collisions as already reported for hard photon emission. The dependence of the impact parameter from the surface of the colliding system was already predicted for high energy gamma emission by BUU calculations [**50**Bauer86] In ref [**106**Lefort00] from the light particles (p, d, t, ^{3}He and ^{4}He) measured in Ar+Ni collisions from 52 to 95 A·MeV the amount of matter and the energy associated with the IS are estimated and the results indicate that the total mass is directly correlated to the impact parameter and it doesn't depend on the incident energy while the energy carried by light particles at intermediate velocity is not strongly dependent on the impact parameter but it depends on the incident energy.

We have to mention (see chapter "Neck Dynamics") that recently a lot of work has been concentrate on the isotopic measurements of IMF (Z≥3) emitted at midvelocity in order to study the nature of the "neck" formation. More neutron rich IMF at midvelocities with respect to the IMF emitted by the projectile-like have been found in the four reactions ^{124,136}Xe + ^{112,124}Sn [**107**Dempsey96] at 55 A·MeV supporting the idea that IMF are emitted from a multiple neck rupture from a material that is "surface-like" thus enhancing the N/Z ratio. This results were confirmed by the chemical analysis of the mid-velocity component measured [**92**plagnol00] in peripheral and semi-central collisions induced by Xe and Sn at energies between 25-50 A·MeV. The results show that the emitted

neutron richest isotopes are favored at lower energies and in peripheral collisions and it is found to be more neutron reach with respect to evaporative processes. Similar results have been found in [**108**milazzo01] where more neutron rich He isotopes are found in mid-peripheral emission from the neck zone respect with He isotopes emitted from PLF. Exclusive measurements of the neutrons and protons emission characteristics from intermediate velocity source, measured in the same reactions with different N/Z ratio, and comparison with dynamical calculations can add information on the mechanism leading to the neutron enrichment of the neck region.

From the analysis of the proton angular distributions in reactions with different mass asymmetry at 44 A·MeV [**12**Coniglione00] a reminiscence of the elementary nucleon-nucleon cross section in the observed anisotropy in central collisions for quasi-symmetric system confirms the hypothesis that pre-equilibrium protons are emitted as consequence of first Nucleon-Nucleon collisions. These results, compared with Boltzmann Nordhaim Vlasov (BNV) predictions, are consistent with a scenario where the particles are emitted in the first phase of the reaction mainly from the first N-N collisions in the interaction zone and candidate protons as probe to study the in-medium nuclear effects of the elementary NN cross section. Due to the short mean free path of protons a strong screening effect is evident, distorting the expected angular distribution trends in peripheral reactions and heavy systems. A clear signature of this scenario is provided by the γ-p correlation results [**68**Sapienza94] as described in the previous section regarding the hard photon production. These results candidate protons, studied in symmetric and light systems, as probes to gather information on the in-medium nucleon-nucleon cross section.

High efficiency apparata are able to measure differential energy spectra that span several orders of magnitude putting in evidence the presence of particles with energy per nucleon up to 3-4 times the incident energy per nucleon [**109**Germain97,**12**coniglione00,**3**wada04,**13**sapienza01]. In the hypothesis that energetic protons are emitted as consequence of first chance NN collisions and sharp Fermi momentum distributions the presence of a kinematical limit in the proton energies is expected. The observation in the energy spectra of protons far exceeding this limit is a puzzle not yet resolved and can ascribe the emission of extremely energetic nucleons as deep subthreshold emission. The mechanisms able to concentrate in few nucleons so much energy is not yet known but its knowledge can be of crucial importance to shed light on the sub-thresholds particle emission mechanism in heavy ion reaction at intermediate energy. Mechanisms as cooperative effects [**15**Bonasera94], high momentum tail of the nucleon Fermi distribution [**110**Bobeldijk95], fluctuations in the momentum-space [**111**Germain98] or properties of the potential have been addressed as responsible of energetic particles production. Attempts to reproduce the extremely high energy tail in proton spectra with dynamical model predictions [**3**wada04,**13**sapienza01,**109**germain97,**111**germain98] that include also different prescription for the effective mean field potential and in medium properties of the two body collisions cross section have been done. The most promising mechanisms responsible for the production of extremely energetic protons seems to be a cooperative mechanism where more nucleons act together to produce an high energy nucleon. Also in the emission of high energy gamma a kinematical limits for n-p collisions is expected and high energy gamma exceeding this limit has been observed in ref [**81**Gudima96].

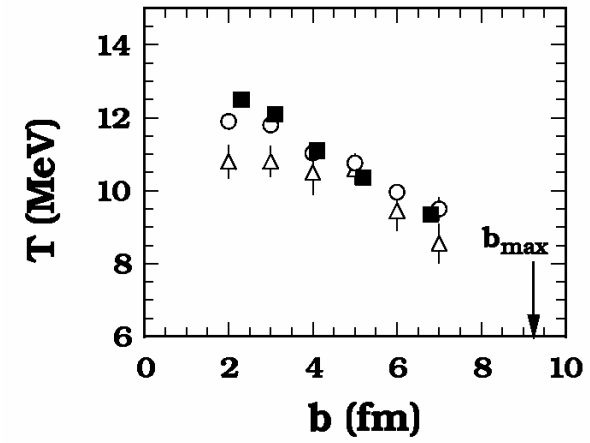

Fig.- 14- Inverse slope parameters extracted from proton spectra as a function of the impact parameters for the $^{58}Ni+^{58}Ni$ at 30 A·MeV. Full squares represent the experimental data, open triangles the BNV calculations with a local mean field and open circles the BNV calculations with a momentum dependent potential [**112**Sapienza04]

Experimental inclusive proton spectra measured in the Ar+Ta at 95 A·MeV at large polar angles [**109**Germain97] were compared with BNV calculations that include beside the usual local mean field potential and two body collisions, three body collisions which succeeded in the explanation of sub-threshold pions production (see section on pions). The comparison with the experimental data shows good agreement in the reproduction of the high energy slope. The same experimental data was examined in ref [**111**germain98] and compared with QMD calculations in which collective effects were introduced. In this case the simulations overestimated the data leading the authors to the conclusions that high collective effects are not necessary to explain the data. These contradictory conclusions are a clear indication that models have to be improved and comparison with exclusive experimental data are needed.

An effort in this sense has been carried out measuring proton up twice the NN kinematical limit (5 times the beam energy per nucleon) as a function of the centralities in the $^{58}Ni+^{58}Ni$ reaction at 30 A·MeV. The slope and yield of energetic proton spectra collected at different impact parameters were extracted and the comparison with a results of BNV calculations with a local Skyrme potential and Gale-Bertsh-Das Gupta momentum dependent potential is reported in Fig 14 [**112**Sapienza04]. The slope are well reproduced by a momentum dependent potential while the local potential fails especially at central collisions. Since the momentum dependent effects could be expected also from a stiff potential the dependence on the compressibility term has been also investigated for the same reaction [**113**Sapienza01LNSreport]. The proton high energy spectra predicted by BNV calculations with a hard and stiff compressibility value within a local Skyrme interaction have been compared to the experimental spectra and the results indicate that the proton spectra are not sensitive to the compressibility term while they are sensitive, both in yield and slope, to a momentum dependent potential.

A more detailed analysis for the same reaction has been performed in [**13**Sapienza01]. High energy protons were detected in coincidence with heavy fragments in order to select classes of events with different centralities. For each class of events high energy gammas were measured in coincidence and a quantitative measure of the size of the interaction zone (A_{part}) was determined. In Fig. 15 are reported the high energy proton multiplicities as a function of A_{part} (i.e. impact parameter) for different energy proton values. A linear dependence on A_{part} (continuous line in the left panels) is observed for proton between 60 and 80 MeV thus confirming that the high energy proton increases linearly with increasing A_{part}. Increasing the proton energies a stronger and stronger deviation from linearity is observed. The continuous line in the top right figure shows a quadratic dependence. Similar behavior is observed for π° and η at much higher incident energies [**114**Wolf98] and explained as due to multi-step processes. The experimental data were compared with microscopic BNV calculations where two different potentials were included: a local Skyrme interaction (open squares in Fig 15) and a Gale-Bertsch-Das Gupta momentum dependent interaction (open circles). Momentum dependent BNV calculations explain well the data up to 120 MeV (left panels in Fig.15) while fail reproducing extremely high energy proton multiplicity. BNV with local potential undershoot the data already at low energies and central collisions. These results call for the introduction in the transport models of ingredients that are beyond the one and two body effects as cooperative effects (three or high order collisions). Transport models prediction that take into account local potentials are able to reproduce energy spectra and high energy proton multiplicities for peripheral collisions and inclusive data. This calls for three (or four…) body or more cooperative effects for their production [**15**Bonasera94]. The fact that three body effects might be important has been advocated also in microscopic Bruckner HF calculations [**8**Lombardo02] to reproduce the experimental ground state energy and density of nuclear matter. As we see in this experiment, even though cooperative effects are important, their relevance compared to nucleons produced from two body collisions is negligible. In the BHF microscopic calculations instead the relevance of the three body force is large, in fact the ground state density in the calculations decreases almost of a factor two when three body forces are included (**8**Lombardo02,**115**BonaseraCortona05). We would expect that when increasing the excitation energy of the system three body forces would become even more important as compared to the cold nuclear matter because of some relaxation of the Pauli blocking (density dependence). This does not seem to be the case and even though three body effects could explain the data, they are absolutely negligible compared to the

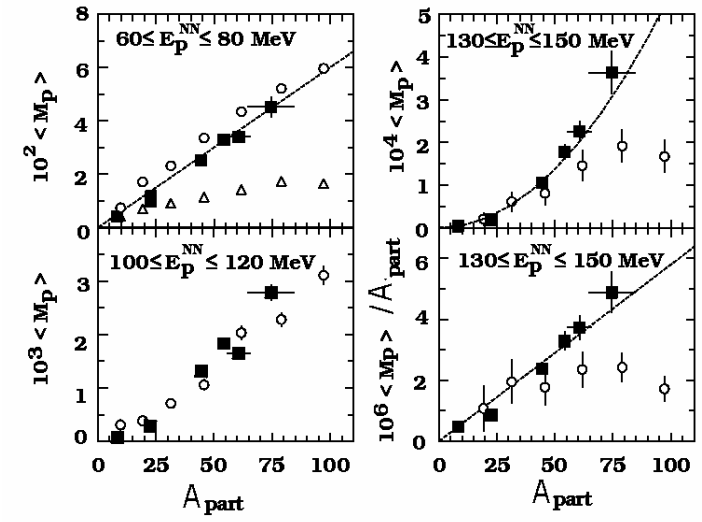

Fig-15-. Proton multiplicities as function of the number of participant nucleons (A_{part}) for different proton energies in the $^{58}Ni+^{58}Ni$ at 30 A·MeV. Full squares represent experimental data, open triangles BNV calculation results with a local potential and open circles BNV calculation with a momentum dependent potential. In the bottom right panel the points for $130 \le E_p \le 150$ MeV are reported divided by A_{part}. The BNV calculations are scaled by a factor 0.6 in order to take into account the yield reduction due to the complex particle emission not predicted by the calculations [**112**sapienza04].

main part of the spectrum which is associated to two body collisions. This aspects calls for a further and more detailed experimental and theoretical analysis of these reactions at various beam energies to try to pin down the relevance of two body versus three body forces which could be relevant for microscopic calculations of the nuclear matter EOS and the binding energies of light nuclei.

Recently, a detailed comparison between experimental results from several reaction at different incident energies (^{64}Zn + ^{58}Ni, ^{92}Mo and ^{197}Au at 26,35,47 A·MeV) with dynamical model predictions have been presented in ref [**3**Wada2004]. Direct experimental observable as velocity and energy spectra, multiplicity and charge distribution for light particles (p, d, t, α) and Intermediate Mass Fragment (Z≥3) have been compared with a modified Antisymmetrized Molecular Dynamics prediction (AMD-V) that take into account different prescriptions for the in-medium N-N cross section and a Gogny effective interaction with a momentum dependent mean field and two different compressibility values. The general aim of that work is to get information on the reaction mechanisms comparing the model results with a wide set of experimental data. In Fig. 12 are reported the experimental proton energy spectra (dots) and AMD-V calculations results with two different compressibility values and in-medium NN cross section description. In Fig. 12 results corresponding to a compressibility for infinite nuclear matter K=228 MeV and an empirical in-medium NN cross section prescription where no distinction is made between n-n and n-p cross sections (soft EOS+NN_{emp}) are represented as thick lines while results corresponding to K=360 MeV and an in-medium NN cross section with different cross section prescription for n-n and n-p cross sections (stiff EOS+NN_{LM}) are represented as thin lines. The calculation results which take into account a stiff EOS and soft EOS are both in qualitative agreement with the bulk of data presented but are not able to reproduce the high proton energy tails (see Fig 12) especially at around 50° polar angle, which corresponds to emission near 90° in the center of mass system, where the high energy IS component can be clearly evidenced. Comparison between data and calculation results taking into account free NN cross section was not shown by the authors.

CONCLUSIONS AND FUTURE PERSPECTIVES

In this work we have reviewed the production of subthreshold π, hard photons and energetic nucleons in nucleus-nucleus collisions at intermediate energies (10 A·MeV ≤ E/A ≤ 100 A·MeV). A first remark concerns the fact that the bulk of data are qualitatively rather well reproduced by dynamical calculations like BUU, where the nuclear dynamics are described in terms of mean field and two body collisions, thus confirming the dominant role of nucleon-nucleon collisions, whose energy is boosted by the presence of the Fermi motion of the colliding nuclei, for the production of these "particles". This result opened the possibility of carrying on a more detailed comparison between experimental data and calculations in order to put constraints on basic ingredients of the theoretical model and therefore on the equation of state of nuclear matter. Another issue concerns the fact that the understanding of the main production mechanisms for high energy particles and its general agreement with calculations of dynamical transport models, qualify these "particles" as probes for the early non equilibrated stage of the reaction allowing to extract information about this particular phase and on the following evolution towards equilibration. In particular the dependence on the nuclear compressibility, on the momentum dependence of the nuclear mean field, on nucleon-nucleon cross section in medium, etc., can be tested. Some interesting results from a detailed comparison between data and calculations have been obtained:

- evidence for effects due to momentum dependent interactions (observed, for example, in the case of energetic proton production);
- particle production is of course very sensitive to the NN cross section (an effect has been observed in the angular distributions of energetic protons), however more work should be done to draw conclusive answers on the σ_{NN} modification in the nuclear medium taking also into account the effects on the reaction dynamics;
- the features of the nuclear dynamics from a large amount of data, especially concerning light particles and IMF emission both in peripheral and central collisions, are well described by dynamical calculations only for a soft EOS (i.e. neck emission, multifragmentation with particular reference to IMF-γ correlation, …).

However, the agreement between data and calculations and the possibility to put constraints on basic ingredients, that can improve the understanding of the EOS, could be weakened by the presence in the models of many parameter to be tuned such as the width of the Gaussians or the cell sizes if delta functions are used for the test particles. In particular in models should be tested the real mean field properties used which could be different if using one prescription or another for the test particles representation. Other physical quantities such as the surface term should be more deeply investigated for instance by comparing the same transport codes to fusion or deep inelastic reactions at energies near the Coulomb barrier. In this respect the approach of the chapter "Comparison of

Transport Codes" seems very promising and should be extended to the items discussed in this chapter. Therefore one main suggestion could be to compare the results of several dynamical calculations with many different experimental data, for example for both energetic nucleon, π and hard photon production and on the other hand to verify that the same prescriptions allow also a good description of other features of the nucleus-nucleus dynamics both in peripheral (neck, PLF fragmentation, etc.) and central collisions (fusion, multifragmentation, etc.). This procedure should allow to really constrain the parameters of interest for the EOS. Moreover, the fact that a probe is sensitive only to some parameters of the EOS and not to others is important since it allows to disentangle between the contribution of various parameters. This is the case of hard photons and energetic nucleon spectra which are not particularly sensitive to the stiffness of the EOS. However, for energetic proton production, a strong improvement in the agreement between data and calculations is achieved, for central collisions, only including a momentum dependence of the nuclear mean field interaction. To our knowledge, momentum dependent calculations have not been carried out for the hard photon production and since the effect of Pauli in the final state is much stronger in this case, this comparison is expected to provide additional valuable information. Moreover, hard photons, which are imperturbed probes due to the fact that they once produced do not interact anymore with the surrounding nuclear matter, provide a clean cronology at various stages of reaction. In particular, energetic hard photons ($E_\gamma > 50$ MeV) gave access to the momentum Fermi distributions of the colliding nuclei in the early non equilibrated stages of the reaction, while the “thermal” hard photons provide a clock for the occurring of multifragmentation in nucleus-nucleus collisions at bombarding energy per nucleon above the Fermi energy. Concerning the comparison with models, with particular reference to the elementary nucleon-nucleon bremsstrahlung cross sections, one should also take into accounts the results of recent experiments which studied the proton induced reactions at 190 MeV on a liquid hydrogen target [**116**Huis99], where high pp bremsstrahlung data has been obtained, and on a deuterium target [**117**Vol03, **118**Vol04], where all the channels leading to gamma bremsstrahlung, including the coherent bremsstrahlung contribution, have been investigated and compared with several theoretical models.

The observation of deep-subthreshold or extremely energetic "particles" addressed the question of which mechanisms could allow to concentrate a relevant fraction of the available energy in the production of a single energetic or massive "particle". For hard photons, pions and energetic protons as described in this report, as far as we know, there is a lack of theoretical models to compare with existing deep subthreshold data. Cooperative effects, where more nucleons or cluster of nucleons participate in the collisions, seems very promising and more theoretical effort should be devoted to this issue. One extreme case which we would like to stress is pionic fusion where all the beam energy is transformed into the pion mass and a compound nucleus is formed very close to its ground state [**119**Horn96].

In the near future the investigation of the isospin degree of freedom will be boosted by the new facilities providing exotic beams and its impact on the EOS of asymmetric nuclear matter will be the next challenge for heavy ion nuclear physics. In this field, n, p, pion and hard photon detection is expected to provide very important pieces of information, especially due to the fact that these probes are sensitive to the first stage of the reaction where the largest asymmetry in isospin and densities can be reached.

In asymmetric matter a splitting of neutron and proton effective masses is expected, but the sign of the splitting is quite controversial giving opposite results for various Skyrme forces. The investigation of pre-equilibrium particles, where the high momentum components have a crucial role, could provide sensitive probes. In particular the N/Z of fast nucleon emission as a function of centrality and the slopes and yields of hard photon spectra, which can provide complementary pieces of information with respect to the nucleon emission thanks to the fact that they are not affected by final state interaction, should be carried out [**120**Spi05].

Concerning the pion emission, several theoretical works have been published investigating the sensitivity of the π^+/π^- ratio to the isospin degree of freedom at incident energies of about 400 AMeV and the dependence on the neutron and proton chemical potentials and on the symmetry energy have been put in evidence [**121**BALi03, **122**Gai04]. However, it is important to underline that these works deal with equilibrated dense nuclear matter, while the possibility of investigating the π^+/π^- ratio at incident nucleon energy below the nucleon-nucleon pion energy threshold, could give access to the early non equilibrated stage of the reaction.

REFERENCES

1. Migneco E. et al., Nucl. Instrum. Methods. Phys. Res. A314, 31-55(1992)

2. Pouthas J. et al., Nucl. Instrum. Methods. Phys. Res. A357, 418-442(1995)
3. Wada, R., et al., Phys. Rev.C69, 044610 (2004)
4. Pagano A. et al., Nucl. .Phys. A681,331 (2001)
5. Martinez G. et al., Nucl. Instrum. Methods. Phys. Res. A391, 435 (1997)
6. De Souza R. T. et al., Nucl. Instrum. Methods. Phys. Res. A295, 109-122 (1990)
7. Iori I. Et al., Nucl. Instrum. Methods. Phys. Res. A325, 458 (1993)
8. Zuo W, Lejeune A, Lombardo U, et al., Eur. Phys. J. A 14, 469(2002); Zuo W., Lejeune A., Lombardo U., et al. Nucl. Phys. A706, 418 (2002).
9. Kievski A. proceedings of the 10th Conference on Problems in Theoretical Nuclear Physics, Cortona 6-9 October 2004, Worls Scientific
10. Bonasera A., Bruno M., Dorso C.O.and Mastinu P.F., Rivista Nuovo Cimento 23,n.2, 1 (2000).
11. Povh, Rith, Scholz and Zetsche, Particles and Nuclei – An introduction to the Physical Concepts, Edited by Springer
12. Coniglione, R., et al., Phys. Lett. B471, 339-345 (2000)
13. Sapienza, P., et al., Phys. Rev. Lett. 87, 072701 (2001)
14. Cassing W. et al., Phys. Rep. 188,365 (1990)
15. Bonasera A., Gulminelli F. and Molitoris J., Phys Rep.243, 1-124 (1994)
16. Bertsch G. F. and Das Gupta S., Phys Rep.160, 189 (1988)
17. Aichelin J., Phys.Rep.202, 233 (1991)
18. Julien J. et al., Phys. Lett. B264 269-273 (1991)
19. Aichelin J. and Bertsch G., Phys. Lett. B 138, 350-352 (1984).
20. Shyam R. and Knoll J., Nucl. Phys. A426, 606-624 (1984)
21. Bonasera A. and Bertsch G.F. Phys. Lett. B 195, 521-523 (1987)
22. Bauer W., Phys. Rev. C40, 715-718 (1989)
23. Badalà et al., Phys. Rev. C48, 2350-2354 (1993)
24. Benenson W. et al., Phys. Rev: Lett. 43, 683 (1979)
25. Young G.R. et al., Phys. Rev. C33, 742-745 (1986)
26. Kwato Njock M. et al., Nucl Phys. A489, 368-380 (1988)
27. Metag V., Nucl. Phys. A488, 483c-502c (1988)
28. Feldmeier H. and Schnack J., Rev. Mod. Phys. 72, 655-688 (2000)
29. Ono A. et al., Phys. Rev. Lett. 68, 2898-2900 (1992)
30. Papa M., Maruyama T. and Bonasera A., Phys.Rev. C 64, 024612 (2001)
31. Lacroix D. and Chomaz Ph.,Nucl.Phys. A636, 85-110 (1998)
32. Bonasera ArXi –nucl-th/0110068
33. Kodama T. et al., Phys. Rev. C29, 2146 (1984)
34. Bonasera A. and Gulminelli F., Phys.Lett. B 275,24 (1992)
35. Danielewicz P., Pan Q. Phys.Rev. C 46, 2002 (1992)
36. Aichelin J., Ko C.M., Phys. Rev. Lett. 55, 2661 (1985).
37. Badalà A. et al., Phys.Rev.C54,2138-2142(1996).
38. Badalà A. et al., Phys.Rev.C57, 166-167 (1998).
39. Piattelli P. et al., Nucl. Phys A649,181c (1996)
40. Snover K. A., Ann. Rev. Nucl. Part. Sci. 36, 545-603 (1986)
41. Gardoje J. J.,Ann. Rev. Nucl. Part. Sci. 42, 483-536 (1992)
42. Le Faou J.H. et al., Phys.Rev.Lett.72, 3321(1994)
43. Noll H., et al., Phys. Rev. Lett. 52, 1284 (1984)
44. Grosse E., Nucl. Phys. A447, 611c (1985); Grosse E. et al., Europhys. Lett. 2, 9 (1986)
45. Gan N. et al., Phys. Rev. C49,298-303 (1994)
46. Clayton J., et al., Phys. Rev. C40, 1207 (1989)
47. Vasak D. et al., Nucl. Phys. A428 (1984)
48. Che Ming Ko, Bertsch G. and Aichelin J., Phys. Rev. C31, R2324-R2326 (1985)
49. Nakayama K. and Bertsch G. F., Phys. Rev. C36, 1848-1852 (1987)
50. Bauer W. et al., Phys. Rev. C34, 2127-2133 (1986) and Biro T. S. et al., Nucl. Phys. A475, 579-597 (1987)
51. Remington B.A., Blann M. and Bertsch G. F., Phys. Rev: Lett. 57, 2909-2911 (1986) and Remington B. A. and Blann M., Phys. Rev. C36, 1387-1396 (1987)
52. Jackson J.D. , Classical Electrodynamics, Edited by J.Wiley & Sons
53. Cassing W. et al Phys. Lett. B181, 217-222 (1986)
54. Nakayama K., Phys. Rev. C42, 1009(1989)
55. Herrmann N. et al., Phys. Rev. Lett. 60, 1630-1633 (1988)
56. Nifenecker H. and Bondorf J. P., Nucl. Phys. A442, 478 (1985) and Nifenecker H. and Pinston J. A., Ann. Rev. Nucl. Part. Science 40 (1990)
57. Shyam R. and Knoll J., Nucl. Phys. A448, 322-332 (1986)
58. Stevenson J. et al., Phys. Rev. Lett. 57, 555-558 (1986)
59. Breitbach G. et al., Phys. Rev. C40, 2893-2896 (1989)

60. Tam C. L. et al., Phys. Rev. C38, 2526-2530 (1988)
61. Alamanos N. et al., Phys. Lett. 173B, 392 (1986)
62. Hingmann R. et al., Phys. Rev. Lett. 58, 759-762 (1987)
63. Reposeur T. et al., Phys. Lett. B276, 418-422 (1992)
64. Riess S. et al., Phys. Rev. Lett. 69, 1504-1507 (1992)
65. Migneco E., et al., Phys. Lett. B298, 46-49 (1993)
66. G. Martinez et al., Phys. Lett. B334 (1994) 23-28
67. Lampis A.R. et al., Phys. Rev. C38 (1988)
68. Sapienza P. et al., Phys. Rev. Lett. 73, 1769-1772 (1994)
69. Badalà A. et al., Phys. Rev. Lett. 74,4779-4782 (1995)
70. Barz H. W. et al., Phys. Rev. C53, R553-R557 (1996)
71. Van Pol J. H. G. et al., Phys. Rev. Lett. 76, 1425-1428 (1996)
72. Piattelli P. et al., Phys. Lett. B442, 48-52 (1998)
73. Viola V. E. Jr. et al., Phys. Rev. C 26, 178 (1982)
74. Schubert A. et al, Phys. Rev. Lett. 72, 1608-1611 (1994)
75. Marqués F. M. et al, Phys. Lett. B 349, 30-34 (1995)
76. Martinez G. et al., Phys. Lett. B 349, 23-29 (1995)
77. D'Enterria D. G. et al., Phys. Rev. Lett. 87, 022701-1 (2001)
78. Alba R. et al., Nucl. Phys. A654, 761c-764c (1999)
79. R. Alba et al., Nucl. Phys. A681 (2001) 339c-342c and R. Alba et al., Nucl. Phys. A749 (2005) 98c-101c and R. Alba et al., submitted to Phys.Rev.Lett. (arXiv:nucl-ex/0507028 22-july-2005)
80. D'Enterria D. G. et al, Phys. Lett. B 538, 27-32 (2002)
81. Gudima K. K. et al., Phys. Rev. Lett. 76, 2412-2415 (1996)
82. Awes, T. C. et al., Phys. Lett. B 103, 417-421 (1981) and Awes, T. C., et al., Phys. Rev. C 24, 89-110 (1981)
83. Awes, T. C., et al., Phys. Rev. C 25, 2361-2390 (1982)
84. Westfall, G. D., et al., Phys. Lett. B 116, 118-122 (1982) and . Westfall, G. D., et al., Phys. Rev. C29, 861-863 (1984).
85. Jacak, B. V., et al., Phys. Rev. C 35, 1751-1788 (1987)
86. Fukuda, T., et al., Nucl. Phys.A 425, 548-572 (1984)
87. Alba, R., et al., Phys. Lett. B 322, 38-42 (1994)
88. Santonocito, D., et al., Phys. Rev.C 66, 044619 (2002)
89. Wada, R., et al., Phys. Rev. C 39, 497-515 (1989)
90. Hasselquist, B. E., Phys. Rev. C 32, 145-162 (1985)
91. Pawloswski, P., et al., Eur. Phys. J. A 9, 371-383 (2000) and reference therein.
92. Plagnol, E., et al., Phys. Rev.C 61, 014606 (2000)
93. Fucks, H., and Mohring, K., Rep. Prog: Phys. 57,231 (1994)
94. Larochelle Y. et al., Phys. Rev. C 59, R565-R569 (1999)
95. Thieriault D. et al., Phys. Rev. C71, 014610 (2005)
96. Ghetti R. t al., Nucl. Phys.A 674, 277-297 (2000)
97. Jacak, B. V., et al., Phys. Rev. C 31, 704-706 (1985)
98. Hagel., K., et al., Phys. Rev.C 62, 034607 (2000).
99. Avdeichikov., V., et al., Nucl. Phys.A 736, 22-38 (2004)
100. Milazzo, P.M., et al., Nucl. Phys. A 756, 39-53 (2005) and De Filippo E. et al., Phys. Rev.C 71, 044602 (2005) and reference therein
101. Kuhrts C. et al., Phys.Rev.C63,034605 (2001)
102. Ghetti, R., et al., Phys. Rev. Lett. 87, 102701 (2001).
103. Verde, G., et al., Phys. Rev.C 65, 054609 (2002).
104. Peter J. et al., Phys.Lett. B 237, 187-191 (1990)
105. Prindle D. et al., Phys. Rev.C 48, 291-307 (1993)
106. Lefort, T., et al., Nucl. Phys.A 662, 397-422 (2000).
107. Dempsey J.F. et al., Phys. Rev.C54, 1710-1718 (1996)
108. Milazzo, P.M., et al., Phys. Lett. B 509, 204-210 (2001)
109. Germain, M., et al., Nucl. Phys. A 620, 81-90 (1997).
110. Bobeldijk I. et al., Phys. Lett. B 353,32 (1995)
111. Germain M., et al., Phys. Lett. B 437, 19-23 (1998)
112. Sapienza P., et al., Nucl. Phys.A 734, 601-604 (2004).
113. Sapienza P. et al., LNS Activity Report 2001, pag 46 www.lns.infn.it
114. Wolf, A. R., et al., Phys. Rev. Lett. 80, 5281 (1998).
115. Bonasera A. pag 171"Proceedings of the 10th Conference on Problems in Theorethical Nuclear Physics", 6-9 October 2004, Edited by World Scientific
116. Huisman H. et al, Phys. Rev. Lett. 83, 4017-4020 (1999)
117. Volkerts M. et al, Phys. Rev. Lett. 90, 062301-1-4 (2003)
118. Volkerts M. et al, Phys. Rev. Lett. 92, 202301-1-4 (2004)